X-RAY SPECTRAL FORMATION IN A CONVERGING FLUID FLOW: SPHERICAL ACCRETION INTO BLACK HOLES

Lev Titarchuk[1,4], Apostolos Mastichiadis[2], and Nikolaos D. Kylafis[3]

Received ______________; accepted ______________

[1]National Aeronautics and Space Administration, Goddard Space Flight Center (NASA/GSFC), Greenbelt, MD 20771, USA; E-mail: titarchuk@lheavx.gsfc.nasa.gov

[2]Max-Planck-Institut für Kernphysik, Postfach 10 39 80, D-69029 Heidelberg, Germany; E-mail: masti@aposto.mpi-hd.mpg.de

[3]University of Crete and Foundation for Research and Technology - Hellas; E-mail: kylafis@physics.uch.gr

[4]George Mason University/Institute for Computational Sciences and Informatics

ABSTRACT

We study Compton upscattering of low-frequency photons in a converging flow of thermal plasma. The photons escape diffusively and electron scattering is the dominant source of opacity. We solve numerically and approximately analytically the equation of radiative transfer in the case of spherical, steady state accretion into black holes. Unlike previous work on this subject, we consider the inner boundary at a *finite* radius and this has a significant effect on the emergent spectrum. It is shown that the bulk motion of the converging flow is more efficient in upscattering photons than thermal Comptonization, provided that the electron temperature in the flow is of order a few keV or less. In this case, the spectrum observed at infinity consists of a soft component coming from those input photons which escaped after a few scatterings without any significant energy change and of a power law which extends to high energies and is made of those photons which underwent significant upscattering. The luminosity of the power law is relatively small compared to that of the soft component. The more reflective the inner boundary is, the flatter the power-law spectrum becomes. The spectral energy power-law index for black-hole accretion is always higher than 1 and it is approximately 1.5 for high accretion rates. This result tempts us to say that bulk motion Comptonization might be the mechanism behind the power-law spectra seen in black-hole X-ray sources.

Subject headings: accretion — black hole physics — radiation mechanisms: Compton and inverse Compton — radiative transfer — stars: neutron — X-rays: general

1. INTRODUCTION

The problem of Compton upscattering of low-frequency photons in an optically thick, converging flow has been studied by several researchers. Blandford and Payne were the first to address this problem in a series of three papers (Blandford & Payne 1981a,b, hereafter BP81a and BP81b respectively; Payne & Blandford 1981, hereafter PB81).

In the first paper of the series they derived the Fokker-Planck radiative transfer equation which took into account photon diffusion in space and energy, while in the second paper they studied the acceleration of photons in a radiation-dominated, plane-parallel shock by using the Fokker-Planck formalism developed in the first paper. In the third paper they solved the Fokker-Planck radiative transfer equation in the case of steady state, spherically symmetric, super-critical accretion into a central black hole with the assumption of a power-law flow velocity $v(r) \propto r^{-\beta}$ and neglecting thermal Comptonization. For the inner boundary condition they assumed adiabatic compression of photons as $r \to 0$. Thus, their flow extended from $r = 0$ to infinity. They showed that all emergent spectra have a high-energy, power-law tail with index $\alpha = 3/(2 - \beta)$ (for free fall $\beta = 1/2$ and $\alpha = 2$), which is independent of the low-frequency source distribution.

In a extension of the work of BP81b, Lyubarskij & Sunyaev (1982, hereafter LS82) studied Comptonization in a radiation-dominated shock, taking into account not only the bulk motion of the electrons but also their thermal motion. Also Colpi (1988, hereafter C88) generalized the work of PB81 by including the thermal motion of the electrons along with their bulk motion. However, as in PB81, the inner boundary condition was taken at $r = 0$ and thus neglected the black-hole horizon.

The LS82 study was further extended numerically by Riffert (1988, see also the related work by Bekker 1988), who found a self-consistent solution for the photon spectrum, the velocity and the temperature profile in the infinite shock. The spectra derived there

exhibit all the range of features from the thermal Comptonization dominated case to the bulk motion dominated one. Mastichiadis & Kylafis (1992, hereafter MK92) studied the upscattering of low frequency photons in an optically thick, spherical accretion onto a neutron star due to bulk motion only. The effects of the radiation force on the flow and thermal Comptonization were neglected, while the neutron-star surface was considered to be entirely reflective. They showed that the high-energy part of the emergent spectrum is a power-law with energy spectral index essentially zero. No high-energy cutoff was found because the Compton degradation term was not included in the radiative transfer equation.

In the present work we give an accurate numerical and an approximate analytical solution of the problem of spectral formation in a converging flow, which takes into account the inner boundary condition, the free fall motion and the thermal motion of the electrons. The inner boundary is taken at a *finite* radius and the spherical surface there is considered to be anything from fully reflective to fully absorptive. The fully absorptive inner boundary mimics a black-hole horizon. No relativistic effects (special or general) are taken into account in this work and thus our spectra, though very suggestive, make instructive sense only, without being directly comparable with observations. However, our work derives for the first time the spectral-energy power-law index as a function of accretion rate. It demonstrates by using numerical and analytical techniques that the extended power laws are present in the resulting spectra. Thus, it constitutes a significant step towards an exact treatment of Comptonization in matter accreting onto compact objects. Some of the results presented here have already appeared elsewhere (Titarchuk, Mastichiadis & Kylafis 1996).

In § 2 we give a qualitative discussion of the problem to be solved and of the solution that we have obtained. In § 3 we solve numerically and approximately analytically the radiative transfer equation and discuss the properties of the emergent spectrum. Finally, we summarize our work and draw conclusions in § 4.

2. QUALITATIVE DISCUSSION

2.1. Accretion Flow

Let $\dot{M}$ be the rate at which matter is accreting and let its radial inward speed be

$$v_b(r) = c \left[\frac{r_s}{r}\right]^{1/2} \ , \tag{1}$$

where c is the speed of light and r_s is the Scwarzschild radius. This free-fall velocity profile makes the tacit assumption that the radiation force on the accreting matter is insignificant, or equivalently, the escaping luminosity is much less than the Eddington value. The Thomson optical depth of the flow from some radius r to infinity is given by

$$\tau_T(r) = \int_r^\infty dr n_e(r)\sigma_T = \dot{m} \left[\frac{r_s}{r}\right]^{1/2} \ , \tag{2}$$

where $n_e(r)$ is the electron number density, σ_T is the Thomson cross section, $\dot{m} = \dot{M}/\dot{M}_E$ and $\dot{M}_E$ is the Eddington accretion rate defined by

$$\dot{M}_E \equiv \frac{L_E}{c^2} = \frac{4\pi G M m_p}{\sigma_T c} \ , \tag{3}$$

where L_E is the Eddington luminosity, M is the mass of the central object, m_p is the proton mass and G is the gravitational constant. We remark here that $\dot{M}$ can be significantly larger than $\dot{M}_E$, while the escaping luminosity L remains much less than L_E, because the efficiency of converting accretion energy into luminosity is significantly less than unity for radially accreting black holes. Thus, our assumption in equation (1) of a free-fall velocity profile is justified (see also § 3.6 below).

For super-critical accretion into black holes ($\dot{m} \geq 1$), it is evident from equation (2) that there should be regions in the flow from which the photons escape diffusively. Of *qualitative* importance in our discussion is the trapping radius r_{tr} (Rees 1978; Begelman 1979) defined by the relation

$$3\frac{v_b(r_{tr})}{c}\tau_T(r_{tr}) \equiv 1 \ . \tag{4}$$

No *quantitative* importance should be given to the trapping radius, because the mean number of scatterings that photons undergo depends on the photon source distribution.

For our problem it is convenient to use not the Thomson optical depth τ_T but the effective optical depth

$$\tau' \equiv 3\frac{v_b(r)}{c}\tau_T(r) = 3\dot{m}\frac{r_s}{r} \ , \tag{5}$$

defined such that $\tau'(r_{tr}) = 1$. The variable $\tau \equiv \tau'/2$ will replace the radial coordinate r in the radiative transfer equation in § 3.

2.2. Photon Energy Gain and Loss

The physical picture here is the following: Consider a low energy photon that finds itself in the accretion flow. As the photon diffuses outward, it scatters off the inflowing electrons. Since this, in most cases, is an almost head-on collision between a fast moving electron and a low energy photon, the photon gains energy on average. The problem to be solved can then be described qualitatively as follows: Consider a source of photons with frequency ν_0, or a distribution around this frequency, such that $h\nu_0 \ll m_e c^2$. The source of photons is placed anywhere in the accretion flow between the inner and outer boundaries of the flow and with any spatial distribution. For large optical depths in the accretion flow, the photons diffuse in the flow and end up either in the hole or at infinity. For small optical depths (say of order unity), the majority of the input photons escape after a few scatterings without changing their energies significantly (almost coherently scattered). However, a small fraction of the input photons undergo effective scatterings with significant energy change (Hua & Titarchuk 1995). In all cases, the diffusing photons gain energy from the bulk and the thermal motion of the electrons. The objective is to determine the emergent spectrum.

Since the bulk motion involves high speeds, the thermal motion of the electrons has little effect on the emergent spectrum if $kT_e \ll m_e c^2$ (see below for a more quantitative statement). In such a case, the asymptotic behavior of the emergent spectrum is a power-law. The exact value of the power-law exponent depends on the condition at the inner boundary and the accretion rate.

If the inner boundary is fully reflective (MK92), all input photons escape. Furthermore, the repeated reflection of the photons at the inner boundary causes them to scatter many times with the inflowing electrons and the emergent power law is as flat as it can be. For very optically thick flows, the spectral energy power-law exponent is almost zero.

In the opposite case where the inner boundary is fully absorptive, as is the case of a black-hole horizon, the emergent spectrum consists only of the photons that *did not* reach the inner boundary. These photons have had fewer chances to collide with the inflowing electrons and thus the emergent power law is steeper than in the fully reflective case. *The power-law exponent is different than that found by previous workers and this is entirely due to the finite radius of the inner boundary.*

In all cases, the power-law spectrum produced by the bulk motion of the electrons has a cutoff at high energies due to Compton recoil. Below we investigate the relative importance of the bulk (converging flow) and the thermal motion of the electrons to the mean photon energy change per scattering.

There are two contributions to the mean energy gain per scattering of a photon. The first contribution is $< \Delta E_b^{(1)} >$, which is proportional to the first power of v_b/c (BP81a), and is given by (see Appendix D)

$$< \Delta E_b^{(1)} > \approx E \frac{4}{\dot{m}} \ . \tag{6}$$

It is worth noting that an additional factor 1/3 is present in equation (6) in the case of

plane geometry considered by LS82 and Riffert (1988).

The second contribution is proportional to the second power of the electron velocity, i.e., $u^2 = v_{th}^2 + v_b^2$, where v_{th} and v_b are the thermal and bulk velocity respectively, and it is given by (see Appendix D and also eq. [15] of BP81a)

$$< \Delta E_{th,b} >=< \Delta E_{th} > + < \Delta E_b^{(2)} >\approx E\frac{4(kT_e + m_e v_b^2/3)}{m_e c^2} \ . \tag{7a}$$

Thus we have that

$$\frac{< \Delta E_{th} >}{< \Delta E_b^{(1)} > + < \Delta E_b^{(2)} >} \approx \frac{4kT_e}{m_e c^2\{4\dot{m}^{-1} + 4[\tau_T(r)/\dot{m}]^2/3\}} < \frac{1}{\delta} \ , \tag{7b}$$

where

$$\delta \equiv 1/\dot{m}\Theta = 51.1 \times T_{10}^{-1}\dot{m}^{-1} \ , \tag{8}$$

where $\Theta = kT_e/m_e c^2$ and $T_{10} \equiv kT_e/(10 \text{ keV})$. Hence, the bulk motion Comptonization dominates the thermal one if $\dot{m}T_{10} < 51$.

The high-energy cutoff of the spectrum can be understood in the following way: As it is shown in Appendix D, the fractional increase in energy of a low-energy photon in its collision with accreting electrons of bulk velocity v_b and temperature T_e is given by

$$\frac{< \Delta E >_{incr}}{E} \approx 4\dot{m}^{-1} + (4/3)(\tau_T(r)/\dot{m})^2 + \frac{4kT_e}{m_e c^2} \ . \tag{9}$$

At the same time, the recoil effects cause a fractional decrease in the energy of the photon given by (see Appendix D)

$$\frac{< \Delta E >_{decr}}{E} \approx -\frac{E}{m_e c^2} \ . \tag{10}$$

When $E \ll m_e c^2$, the recoil effect is negligible, resulting in a pure power-law spectrum. At high energies and $\dot{m} > 1$ the two effects are comparable and the cutoff in the spectrum occurs at

$$\frac{E_c}{m_e c^2} \approx 4\dot{m}^{-1} + (4/3)(\tau_T/\dot{m})^2 + \frac{4kT_e}{m_e c^2} \ , \tag{11}$$

or $E_c \approx m_e c^2[4/\dot{m} + (4/3)(\tau_T/\dot{m})^2]$ when $kT_e \ll m_e c^2$ and τ_T is an effective Thomson optical depth expected to be less than $\dot{m}$. Because of the high efficiency of the recoil effect at energies of order $m_e c^2$ such photons lose their energy completely after a few scatterings (much less than average).

2.3. Emergent Spectrum

In problems such as ours, the radiative transfer equation can be solved by the method of separation of variables (PB81; C88). Thus, the problem is reduced to finding the eigenvalue and the eigenfunction of the k-component of the solution. In other words, the solution for the occupation number $n(\tau, x)$ is a series of the form

$$n(\tau, x) = \sum_{k=1}^{\infty} c_k R_k(\tau) N_k(x) \ , \tag{12}$$

where τ and x are the space and energy variables respectively, $R_k(\tau)$ is the eigenfunction of the space operator, $N_k(x)$ is the spectrum of the k-mode of the solution and c_k are the expansion coefficients of the space source distribution over the set of the space eigenfunctions $\{R_k(\tau)\}$. For the k-component of the solution [i.e., $c_k R_k(\tau) N_k(x)$], the spectrum $N_k(x)$ *is the same at any place in the converging flow.* We use this modification of the method of separation of variables to find an approximate analytic solution (see §3.3 and Appendix E).

We have solved the radiative transfer equation numerically because an exact solution of the form (12) cannot be found for all energies and because the inner boundary condition depends on energy and also the energy part of the radiative transfer equation (see eq. [14] below) depends on the space variable (optical depth). The numerical solution has shown that the emergent spectrum can be well approximated by an analytic spectrum consisting of two parts. The first is made by those input photons which escape scattered but with negligible change of their energies, while the second is a power law extending to high

energies (see eqns. [21] and [29] below).

3. RADIATIVE TRANSFER

3.1. The Radiative Transfer Equation and its Solution

Now we proceed to write down and solve the radiative transfer equation. Consider spherically symmetric accretion onto a compact object with rate $\dot{m}$. The inflow bulk velocity of the electrons is $\mathbf{v_b}$ and their temperature is T_e. Following BP81a (their eq. [15]), where the bulk motion term v_b^2 is not neglected with respect to the thermal one as it is in their eq. [18]), we write for the occupation number $n(r,\nu)$

$$\frac{\partial n}{\partial t} + \mathbf{v_b} \cdot \nabla n = \nabla \cdot \left[\frac{c}{3\kappa}\nabla n\right] + \frac{1}{3}\nu\frac{\partial n}{\partial \nu}\nabla \cdot \mathbf{v_b}$$
$$+ \frac{1}{\nu^2}\frac{\partial}{\partial \nu}\left[\frac{\kappa h}{m_e c}\nu^4\left(n + \frac{kT_e + m_e v_b^2/3}{h}\frac{\partial n}{\partial \nu}\right)\right] + j(r,\nu) \ , \qquad (13)$$

where h is Planck's constant, $\kappa(r) \equiv n_e(r)\sigma_T$ is the inverse of the scattering mean free path, and $j(r,\nu)$ is the emissivity. Substituting for the inflow velocity $\mathbf{v_b} = -v_b(r)\hat{\mathbf{r}}$, where $\hat{\mathbf{r}}$ is the radial unit vector, and taking into account the spherical symmetry, equation (13) becomes in steady state

$$\tau\frac{\partial^2 n}{\partial \tau^2} - \left(\tau + \frac{3}{2}\right)\frac{\partial n}{\partial \tau} = \frac{1}{2}x\frac{\partial n}{\partial x} - \frac{1}{2\delta_b}\frac{1}{x^2}\frac{\partial}{\partial x}\left[x^4\left(f_b^{-1}n + \frac{\partial n}{\partial x}\right)\right] - \frac{\dot{m}}{2}\frac{j}{\kappa c} \ , \qquad (14)$$

where $x \equiv h\nu/kT_e$, $\tau \equiv \tau'/2$ defined by equation (5) and

$$\delta_b^{-1} \equiv \delta^{-1} f_b(\tau) \ , \qquad (15)$$

where $f_b(\tau) = 1 + (v_b/c)^2/(3\Theta)$.

The dimensionless spectral energy flux $F(r,\nu)$ (PB81, C88) is written in the new variables as

$$F(\tau,x) = x^3\left[\frac{2\tau}{3\dot{m}}\right]^{1/2}\left(\frac{\partial n}{\partial \tau} + \frac{1}{3}x\frac{\partial n}{\partial x}\right) . \qquad (16)$$

Note that the normalization factor $F_0 = 2\pi \times 10^{23}(kT_e/\mathrm{keV})^3 \mathrm{erg\ cm^{-2}s^{-1}keV^{-1}}$ should be introduced in order to express $F(\tau, x)$ in flux units.

There are two boundary conditions which our solution must satisfy. The first is that the total spectral flux integrated over the outer boundary should depend only on x as $\tau \to 0$. Thus,

$$F(\tau_o, x) = C(x)\tau_o^2 \quad \text{as} \quad \tau_o \to 0 \ , \tag{17}$$

where the subscript o means outer boundary. The second boundary condition is that we have a boundary with albedo A at some radius r_b, or equivalently at an effective optical depth τ_b, defined by

$$\tau_b \equiv \frac{\tau_b'}{2} = \frac{3}{2}\frac{v_b(r_b)}{c}\tau_T(r_b) \ . \tag{18}$$

The reason for considering a general albedo A and not only the case $A = 0$ (appropriate for black holes) is to be able to compare our results with those obtained in previous work. The net energy flux through this surface is

$$F(\tau_b, x) = -x^3\left(\frac{1-A}{1+A}\right)\frac{n}{2} \ . \tag{19}$$

¿From the setup of the problem, τ_b is the largest value that the variable τ can obtain.

In a recent preprint, Psaltis and Lamb (1996) rederived the photon kinetic equation for Comptonization, correcting several inaccuracies in the literature. Expansion of the photon kinetic equation in the subrelativistic regime $v_b/c < 1$ over the spherical harmonics leads to equation (14) (or eq. [15] of BP81a) for the zeroth moment of the occupation number.

3.2. Numerical Solution

Equation (14), satisfying the boundary conditions (17) and (19), has been solved numerically and the emergent spectrum has been computed. The method that we used

is the relaxation method for the solution of the boundary problem for elliptic partial differential equations (e.g., Press et al. 1992). The solution of the stationary problem is searched as the equilibrium solution of the approriate initial value problem.

An interesting example of a space source distribution, mimicking the external illumination of a converging flow by the low-energy radiation of an accretion disk, is given by

$$S(\tau) = S_0 \tau^2 \exp(-\tau_T(\tau)/\mu) \ , \tag{20}$$

where S_0 is a normalization constant. An external illumination produces an exponential source distribution over the converging flow. The factor $\tau^2 \propto r^{-2}$ takes into account the space dilution of the radiation, while μ is the cosine of the angle of incidence at $r = r_s$. The physical meaning of this space source distribution is the following: Consider a source of soft photons *outside* the converging flow and at a distance $R_0 \gg r_s$ from the center of the black hole. The source illuminates from the outside the accretion flow and the radiation penetrates with an exponential probability to radius r, where it is isotropized by scattering. Thus, the scattered photons at radius r constitute the source of soft photons that get Comptonized in the accretion flow. We note here that this does not violate the condition of no incoming radiation at the outer boundary. This is a standard procedure for the reduction of the illumination problem to the problem of source distribution within the atmosphere (e.g., Sobolev 1975).

EDITOR: PLACE FIGURE 1 HERE.

A specific example of the emerging spectra, related to the source space distribution (20) and to the source spectral distribution as a blackbody spectrum, is shown in Figure 1. Two of the emergent spectra are presented there. The first one (solid line) is a solution of equation (14) with the appropriate boundary conditions (17) and (19), and δ_b as given by

equation (15). The second spectrum (dashed line) is for the case where the second order effect of the bulk motion has been neglected in the radiative transfer equation. Neglecting the $(v_b/c)^2$ term in equation (14) transforms it into equation (18) of BP81a. It is evident from Figure 1 that the emergent spectral energy flux consists essentially of two components: The first one is due to the majority of the input photons which escape without significant energy change, while the second one is the flux of those relatively few photons which undergo effective repeated scatterings and produce an extended power law. At the same time, the inclusion of the second order bulk effect produces an identical shape of the hard tail (for energies higher than 10 keV) but with a larger photon contribution which, in addition, is extended to higher energies. This is because the second order effect of the bulk motion $(v_b/c)^2$ increases the effectiveness of photon upscattering.

3.3. Analytic Approximation of the Solution

In view of the power-law that is evident in the emergent spectrum in Figure 1, it is natural to seek an approximate analytic solution of equation (14) where a power law is a part of the solution. First, a "solution" of the form (12) (so called Green's function) for equation (14) with the boundary conditions (17) and (19) is derived (for a justification see § 3.4 below). Three assumptions are made in order to separate the energy and space variables (i.e., to present the solution as series [12]).

The first one is that we neglect the bulk motion term $(v_b/c)^2$ in equation (14) which is a function of the space variable τ. It is shown in Figure 1 that the inclusion of this term in the equation does not change the spectral shape of the high-energy part of the spectrum.

The second one is that we assume that the Green's function (i.e., the spectrum for $\delta-$function energy injection) is a power law up to a high energy cutoff. In Appendix B the

energy Green's function is found (eq. [B1]) and the validity of the power-law assumption is demonstrated in Appendix C (see also Fig. 4a, curve 1).

The third one is that, in order to get the complete system of eigenfunctions, we keep the same boundary condition (eq. [A4] of Appendix A) for all of them.

In Appendix A the space eigenvalue problem is solved under these assumptions and the transcendental equation (A6) is derived for the spectral index determination. The approximate analytic solution for the spectral flux can be written as the series (see eqns. [12] and [16])

$$F^{tot}(0,x) = 4\pi r^2 F(0,x) = C_F \sum_{k=1}^{\infty} \frac{c_k}{2\lambda_k^2 - 3} I_k(x,x_0) \ , \tag{21}$$

where

$$C_F = 10\pi r_s^2 (3/2)^{3/2} \dot{m}^{5/2} \ ,$$

c_k are the expansion coefficients of the space source distribution $S(\tau)$ given by equation (B9), λ_k^2 are the eigenvalues of the boundary value problem (A4-A8), while $I_k(x,x_0) = x^3 G_k(x,x_0)$ is the energy Green's function (with $G_k(x,x_0)$ the occupation number Green's function of the Comptonization equation [B1]). In the case where $x_0 \ll 1$ (i.e., the input photon energy $E_0 \ll kT_e$), I_k is given by

$$I_k = \frac{b_k}{2\mu_k x_0} \begin{cases} \left(\dfrac{x}{x_0}\right)^{\alpha_k+3+\delta}, & \text{for } \ x \le x_0; \\ \dfrac{e^{-x}}{\Gamma(2\mu_k)} \left(\dfrac{x}{x_0}\right)^{-\alpha_k} \displaystyle\int_0^{\infty} e^{-t}(x+t)^{\alpha_k+3+\delta} t^{\alpha_k-1} dt, & \text{for } \ x \ge x_0. \end{cases} \tag{22}$$

Here $b_k = \alpha_k(\alpha_k+3+\delta)$, $\mu_k = \frac{1}{2}[(\delta-3)^2 + 8\lambda_k^2\delta]^{1/2}$, and the spectral index is determined by

$$\alpha_k = \frac{1}{2}[(\delta-3)^2 + 8\lambda_k^2\delta]^{1/2} - (3+\delta)/2 \ , \tag{23}$$

The normalization of $I_k(x,x_0)$ is chosen in such a way as to keep the photon number equal to $1/x_0$.

The above relations correspond to a monochromatic photon injection with energy E_0. In order to get the resulting spectrum for an arbitrary source spectrum $g(E_0)$ one has to

convolve this with the energy Green's function. Thus,

$$J_k(E) = \int_0^\infty I_k(E, E_0) g(E_0) dE_0 \ . \tag{24}$$

EDITOR: PLACE FIGURE 2 HERE.

We have checked the numerical versus the approximate analytic solution for a wide range of $\dot{m}$ and blackbody spectra of temperature T_{bb}. In Figure 2 we show a specific example of the emergent spectral energy flux for $\dot{m} = 3$, $kT_e = 1$ keV, $kT_{bb} = 1$ keV and $r_b = r_s$. The solid curve is the emergent spectrum found from the numerical solution of equation (14) without the v_b^2 term and the dashed curve is our approximate analytic solution. As in Figure 1, here also the emergent spectrum consists of two components: a) The bulk of the soft input photons that escaped from the accretion flow without any significant change of their energies. b) A relatively small fraction of the soft photons that is comptonized to high energies and thus forming the extended power law. It is worth noting the discrepancy between the two solutions at the high energy cutoff. Our assumption regarding a power law shape of the Green's function is certainly violated around the high energy cutoff E_c, where the recoil effect becomes important.

3.4. Properties of Emergent Spectra

The upscattered power-law spectrum with the high energy cutoff is accurately described by the first term of series (21). The contribution of the different modes is clearly seen in Figure 3. The high energy part of the spectrum is determined by the first mode only, but the low-energy bump is formed as a result of the summation of all modes.

EDITOR: PLACE FIGURE 3 HERE.

In a realistic situation where radial and disk accretion into a black hole occur simultaneously, expression (20) is only a very rough approximation, but this introduces no qualitative differences in the emergent spectra. A space source distribution of soft input photons different than that in equation (20) affects only the bump of soft photons seen and leaves unaffected the power law. The deeper the soft photons are injected, the smaller the bump. The shallower the injection is, the fewer the photons that get upscattered into the power law (Fig. 4a-b).

EDITOR: PLACE FIGURE 4 HERE.

In Figures 4a and 4b the analytic emergent spectra are presented for different space source distributions. In Figure 4a, curve 1 is for a distribution proportional to the first eigenfunction (eq. [A3], with $\hat{C} = 0$). Curves 2 and 3 are for a distribution appropriate for external illumination (eq. [20]) with illumination cosines $\mu = 1$ and $\mu = 0.3$, respectively. It is evident that the spectral slope of the high-energy power law is independent of the space distribution of low-energy photons and, as we shall show in § 3.5, it is determined by the mass accretion rate $\dot{m}$ only. In addition we want to draw the attention of the reader to curve 1 in Fig. 4a. This curve represents the Green's function (22). It is clearly seen that a pure power law describes the spectrum perfectly over six energy decades. It can also be proved rigorously that, despite the presence of the exponential in front of the integral in equation (22), the power law can extend to $x \gg 1$. As it is shown in Appendix C, the integral in equation (22) is proportional to e^x for $x \lesssim \delta$, while it is proportional to $x^{\alpha_1+3+\delta}$ for $x \gtrsim \delta$. Thus, for $kT_e \ll m_e c^2$, the power law extends to energies of order $m_e c^2$ independently of the electron temperature. For very high energies, $x \gtrsim \delta$, the spectrum exhibits an exponential cutoff.

Now we proceed with the mathematical analysis of the properties of the emergent spectra. The source term $j(\tau, x)$ in the right hand side of equation (14) can be represented in the factorized form $j(\tau, x) = S(\tau)g(x)$ without any loss of generality. For example, $S(\tau)$ can be given by equation (20) and $g(x)$ can be a blackbody spectrum. If one neglects for the moment the energy change in the process of scattering (i.e., assuming coherent scattering), then the radiative transfer equation can be written in operator form as

$$L_\tau n_{coh} = -\frac{\dot{m}}{2}[g(x)/x^3]S(\tau) \ , \tag{25}$$

where

$$L_\tau = \tau\frac{d^2}{d\tau^2} - \left(\tau + \frac{3}{2}\right)\frac{d}{d\tau} \tag{26}$$

is the space operator (see eq. [14]). The solution of this equation with the appropriate boundary condition (A4) is given by the series

$$n_{coh}(\tau) = \frac{\dot{m}}{2}\frac{g(x)}{x^3}\sum_{k=1}^{\infty}\frac{c_k}{\lambda_k^2}R_k(\tau) \ . \tag{27}$$

Thus, the flux reads [cf eq. [21])

$$F_{coh}^{tot}(0, x) = \frac{C_F}{2}\sum_{k=1}^{\infty}\frac{c_k}{\lambda_k^2}g(x) \ . \tag{28}$$

In the case of bulk motion dominated Comptonization, $\lambda_k^2 \gg 3/2$ for all $k \geq 2$ (see, e.g., Fig. 5), and as a result of this the corresponding energy Green functions $I_k(x, x_0)$ are steep and act approximately as $\delta-$functions on the input spectrum. Thus we can approximate the emergent upscattered spectrum as the following combination

$$F^{tot}(0, x) \approx \frac{C_F}{2}c_1\left[\frac{J_1(x)}{\lambda_1^2 - 3/2} - \frac{g(x)}{\lambda_1^2}\right] + F_{coh}^{tot}(0, x) \ , \tag{29}$$

where $J_1(x)$ is given by the convolution shown in equation (24). Equation (29) means that the emergent spectrum can be written approximately as the sum of two components. The first component is the difference between the first terms of the full and the coherent

solutions (i.e., it represents the upscattered component), while the second component is the fully coherent solution.

For the input distribution (20), it is straightforward to derive that the emergent spectral flux is

$$F^{tot}(0,x) \approx F_0 \left\{ c_1 \left[\frac{J_1(x)}{\lambda_1^2 - 3/2} - \frac{g(x)}{\lambda_1^2} \right] + c_{coh} g(x) \right\} , \quad (30)$$

where F_0 is a normalization factor in flux units,

$$c_{coh} = \sum_{k=1}^{\infty} \frac{c_k}{\lambda_k^2} = (2/5)\pi^{1/2} \exp(\eta^2)\ \mathrm{erfc}(\eta) , \quad (31)$$

and

$$\eta = [\dot{m}/6]^{1/2}/\mu . \quad (32)$$

We note here that the approximation of the spectrum presented in equation (29) is valid even if the diffusion approximation is not valid. The only requirement is that the contribution of the upscattering in the emergent spectrum is efficient enough to produce the power-law hard tail. In such a case, the first expansion coefficient c_1 should be found by using the first eigenfunction of the kinetic equation (and not of the Fokker-Planck equation, as in the case of diffusion), while the coherent component $F_{coh}^{tot}(0,x)$ is the emergent spectrum when no energy change occurs during scattering (Titarchuk & Lyubarskij 1995).

3.5. Power-law Spectral Index

In order to obtain the eigenvalues of the space operator, the transcendental equation (A6) is solved numerically and the results are presented in Figure 5. The transcendental equation (A6) is factorized in the limit of $\dot{m} \gg 1$ (see eq. [A8]) and the roots are determined from the factors. The dotted line in Figure 5 is the root of the first factor of equation (A8). As it also can be seen, the solid line and the dotted line perfectly match each other

in the wide range of $1 < \dot{m} \lesssim 15$, while the two start deviating for larger values of $\dot{m}$. This deviation shows the limits of validity and accuracy of the factorization.

EDITOR: PLACE FIGURE 5 HERE.

The asymptotic expression ($\dot{m} \gg 1$) for the root of the first factor of equation (A8) is

$$\lambda_*^2 \approx \frac{3}{2} + \frac{3}{4}\frac{1-A}{1+A}\left[\frac{r_b}{r_s}\right]^{1/2} \quad . \tag{33}$$

In fact this asymptotic expression for λ_*^2 describes the numerical value λ_1^2 with an error of less than 10% (see Fig. 5).

Having obtained the eigenvalues of the space operator, we can calculate the energy spectral index α_1 of the dominant term. As it can be seen from Figure 6a, this quantity demonstrates a weak dependence on the electron temperature for $kT_e \leq 3$ keV. It is evident that in the wide range of $\dot{m}$ ($2 \lesssim \dot{m} \lesssim 15$) we have $1 < \alpha_1 < 1.5$, which is different than what previous workers have found (PB81, C88).

EDITOR: PLACE FIGURE 6 HERE.

For $kT_e \ll m_e c^2$ such that $\delta \gg 1$, equation (23) can be expanded to first order in $1/\delta$, giving

$$\alpha_1 \approx 2\lambda_1^2 - 3 \ , \tag{34}$$

The accuracy of the above formula is better than 10% when the temperature is 1 keV and it becomes better than 1% in the case where the temperature is 0.01 keV.

As long as $\delta \gg 1$, bulk Comptonization effects dominate the thermal ones and the spectral index α_1 of the fundamental mode is weakly dependent on the temperature of the electrons.

Combining equations (33) and (34) we find that for $\dot{m} \gg 1$ and $\delta \gg 1$ the dominant spectral index becomes

$$\alpha_1 \approx \frac{3}{2}\frac{1-A}{1+A}\left[\frac{r_b}{r_s}\right]^{1/2} \quad . \tag{35}$$

with an error of less than 10% for $kT_e = 1$ keV.

The dependence of the spectral index α_1 on the albedo A is displayed in Figure 6b. As we have already pointed out, for $A = 0$ the power-law index is in the range $1 < \alpha_1 < 1.5$ for $\dot{m} \gtrsim 2$. For the fully reflective inner boundary case ($A = 1$), $\alpha_1 \to 0$ for $\dot{m} \gg 1$, as it was found by MK92. For all values of A we have taken $kT_e = 1$ keV and $r_b = r_s$.

It is worth noting that the first term of equation (21) vanishes exponentially when $\tau_b \to \infty$, since the expansion coefficient c_1 goes exponentially to zero. This happens because the normalization H_1 of the fundamental space function $\tau^{5/2}\Phi(-\lambda_1^2 + 5/2, 7/2, \tau)$ (see eqns. [A3], [B9], [B10]) grows exponentially when $\tau_b \gg 1$ (Abramowitz & Stegun 1970). *Thus, series (21) converges to the solution found by PB81 and C88 when* $\tau_b \to \infty$.

3.6. Comptonization Enhancement Factor

A relation can be found between the luminosity of the low-frequency source and the luminosity emerging from the converging flow. Let us use monochromatic, low-frequency, dimensionless, input luminosity with unity normalization, i.e., $L_0 = \int_0^\infty \delta(x - x_0)dx = 1$. The luminosity of any energy component $I_k(x, x_0)$ (eq. [21]) is given by

$$L_k = \int_0^\infty I_k(x, x_0)dx \ . \tag{36}$$

Hereafter the index k has been dropped for simplicity.

One can get by using equation (22) and the integration technique (e.g., Sunyaev &

Titarchuk 1985),

$$L = \frac{L}{L_0} = \alpha(\xi - 1) \begin{cases} \dfrac{1}{\xi(\alpha-1)}\left(1 - \dfrac{\xi}{\xi+\alpha-1}x_0^{\alpha-1}\right), & \text{for } \alpha \geq 1; \\ \dfrac{\Gamma(\xi)\Gamma(\alpha)\Gamma(1-\alpha)(1-x_0^{1-\alpha})x_0^{\alpha-1}}{\Gamma(\alpha+\xi)}, & \text{for } \alpha \leq 1, \end{cases} \tag{37}$$

where $\xi = \alpha + 4 + \delta$. This result is a generalization of the result of Sunyaev & Titarchuk (1980) for the converging inflow case and expression (37) produces a continuous transition through the value $\alpha = 1$.

The important conclusion which can be deduced from equation (37) is that the low-frequency source flux is amplified only by a factor ~ 3 (for $\alpha_1 \approx 1.5$) due to Comptonization in the accretion flow into a black hole. Thus, the effectiveness of the bulk motion Comptonization is rather weak. It is easy to show that the upscattering effect is negligible ($L/L_0 \approx 1$) for the k mode with $k \geq 2$, because the spectral indices $\alpha \geq 2$ (eq. [34] holds for all modes when the temperature does not exceed 1 keV).

In §2 we assumed a free-fall velocity profile. Since the energy gain due to the bulk motion Comptonization is not bigger than a factor of 3, it follows that we can safely neglect the effects of the radiation force in our calculations if the injected photon flux in the converging inflow is of order of a few percent of the Eddington luminosity.

4. DISCUSSION AND CONCLUSIONS

We have studied Compton upscattering in the case of thermal plasma infalling radially into a compact object. The flow is considered to be finite (as opposed to an infinite one considered in the related work of PB81 and C88) by taking as inner boundary a totally absorptive surface to simulate spherical accretion into a black hole. The emergent spectrum is calculated by solving the radiative transfer equation in the diffusion approximation with a soft source of input photons.

We have considered two different expressions of the transfer equation. In the first case we have included the second order effect of the bulk motion (eq. [14]), while in the second case we have neglected it reducing the equation to the one solved in PB81 and C88 –note, however, the different boundary conditions. We have solved the equation in the first case numerically and in the second case both numerically and approximately analytically. While, formally speaking, the second order bulk effect should not be neglected, by comparing our numerical solutions for the two cases we were able to conclude that the inclusion of this effect does not significantly change the properties of the emergent spectrum. Thus solving approximately analytically the transfer equation when the second order bulk effect has been neglected enabled us to study in detail the properties of the emergent spectrum. This spectrum consists of two components, irrespective of the assumptions on the second order bulk effect: The first component consists of those soft input photons that escaped without any significant energy change, while the second is a power law that extends to high energies. The power law spectral index is not sensitive to whether the second order bulk effect is included in the transfer equation or not (see Fig.1). Thus, by using the analytic solution we were able to determine the spectral index as a function of mass accretion rate $\dot{m}$ and we showed that this lies between 1 and 1.5 for a wide range of $\dot{m}$; furthermore we showed that the spectral index is largely independent of the electron temperature as long as this is below 1 keV (Fig. 6a). Therefore we have found that *the finite extent of the converging flow has crucial effects on the emergent spectrum for moderately super-Eddington mass accretion rates.* For extremely large mass accretion rates, our solution tends to the solution found by PB81 and C88.

Our approach cannot determine accurately the exact position of the high energy cutoff. When the second order effect of the bulk motion is included, the numerically obtained spectra show that the cutoff is of order of the electron rest mass. This is further confirmed by Monte-Carlo calculations (Kylafis & Litchfield 1997, in preparation). If the second

order bulk effect is neglected, then the cutoff is of order of $m_e c^2/\dot{m}$ as this is confirmed by numerical and analytical estimates. At any rate, both formalisms show *qualitatively* the same result, i.e., that bulk motion Comptonization produces a power law which extends to very high energies, of order the electron rest mass.

Our spectra hint at what may be happening in candidate black-hole X-ray sources. We find bulk motion Comptonization as an exciting possibility for the formation of extended power laws in the spectra of black-hole X-ray sources.

5. Acknowledgements

We thank Peter Meszaros for reading and evaluating the present paper. We also thank an anonymous referee for comments on an earlier version of this paper. L.T. would like to acknowledge support from an NRC grant, NASA grant NCC5-52 and from Sonderforschungsbereich 328 during his visit to MPIK. N.K. acknowledges support from EU grant CHRX-CT93-0329. L.T. and A.M. thank the staff of the Foundation for Research and Technology-Hellas for their hospitality. Also L.T. thanks Sandip Chakrabarti, John Contopoulos and Thomas Zannias and A.M thanks John Kirk for extensive discussions. This work was partially supported by the Deutsche Forschungsgemeinschaft under Sonderforschungsbereich 328.

A. THE SPACE BOUNDARY CONDITIONS AND THE EIGENVALUE AND EIGENFUNCTION PROBLEM

In this Appendix we solve the radiative transfer equation (14) taking into account the boundary conditions (17) and (19), and under the assumptions stated in § 3.3. We are looking for a general solution of the form

$$n(x,\tau) = R(\tau)N(x) \ . \tag{A1}$$

The space part of equation (14) can be written as

$$\tau\frac{d^2R}{d\tau^2} - (\tau + 3/2)\frac{dR}{d\tau} + \lambda^2 R = 0 \ , \tag{A2}$$

and its solution is (see, e.g., Abramowitz & Stegun 1970)

$$R(\tau) = \hat{C}\Phi(-\lambda^2, 3/2, \tau) + C\tau^{5/2}\Phi(-\lambda^2 + 5/2, 7/2, \tau) \ , \tag{A3}$$

where $\Phi(a,b,z)$ is the confluent (or degenerate) hypergeometric function and $\hat{C}$ and C are arbitrary constants. Here λ^2 are the eigenvalues of the problem, which we determine below. One can show that the boundary condition (17) implies that $\hat{C} = 0$; otherwise, as $\tau \to 0$, $F(\tau, x) \propto \tau^{1/2}$, contrary to equation (17).

In Titarchuk & Lyubarskij (1995) it is proved that a power law is the exact solution of the radiative transfer kinetic equation up to the exponential turnover where downscattering due to the recoil effect becomes important. Thus we assume that the energy part of the first term is a power law $N(x) \propto x^{-\varepsilon_1}$ up to the exponential cutoff. Note that the occupation number spectral index ε_1 is related to the index α_1 of the spectral energy flux by $\varepsilon_1 = \alpha_1 + 3$ (see, e.g., eq. [19]). The boundary condition (19) implies for $R_1(\tau)$ at $\tau = \tau_b$ that

$$\frac{dR_1}{d\tau} - \frac{\hat{\varepsilon}_1}{3}R_1 = 0 \ , \tag{A4}$$

where

$$\hat{\varepsilon}_1 = \varepsilon_1 - \frac{3(1-A)}{2(1+A)}\left[\frac{r_b}{r_s}\right]^{1/2} \ . \tag{A5}$$

This boundary condition, along with equation (A3), implies that the eigenvalues are the roots of the equation

$$\left(\frac{5}{2}-\frac{\hat{\varepsilon}_1}{3}\tau_b\right)\Phi(-\lambda^2+5/2,7/2,\tau_b)+\frac{5-2\lambda^2}{7}\tau_b\Phi(-\lambda^2+7/2,9/2,\tau_b)=0\ . \qquad \text{(A6)}$$

This can be further written as

$$\Phi(-\lambda^2+5/2,7/2,\tau_b)\left[\left(\frac{5}{2}-\frac{\hat{\varepsilon}_1}{3}\tau_b\right)+\frac{5-2\lambda^2}{7}\tau_b\frac{\Phi(-\lambda^2+7/2,9/2,\tau_b)}{\Phi(-\lambda^2+5/2,7/2,\tau_b)}\right]=0\ . \qquad \text{(A7)}$$

Using the asymptotic form of the confluent hypergeometric function $\Phi(a,b,z)$ for large argument $z \gg 1$ (Abramowitz and Stegun 1970, eq. [13.1.4])

$$\Phi(a,b,z)=\frac{\Gamma(b)}{\Gamma(a)}e^z z^{a-b}[1\ +\ O(z^{-1})]\ ,$$

and representing $\Gamma(a)$ as the product

$$\Gamma(a)=\Gamma(a+n)/\prod_{i=0}^{n-1}(a+i) \qquad \text{for } n=1,2,...,$$

we obtain the asymptotic form of equation (A7) which is valid for $\tau_b \gg \lambda^2$

$$\left(\frac{\hat{\varepsilon}_1}{3}-1+O(\tau_b^{-1})\right)\prod_{n=2}^{\infty}\left(\frac{2n+1}{2}-\lambda_n^2\right)=0\ . \qquad \text{(A8)}$$

¿From the first term of the product we get $\hat{\varepsilon}_1 \approx 3$ which implies (eq. [A5]) $\varepsilon_1 \approx 3+1.5[(1-A)/(1+A)](r_b/r_s)^{1/2}$. The other roots 5/2, 7/2, ..., (2n+1)/2, ... are related with the second, third and nth term of the above product respectively.

Two more steps are required to calculate the emergent spectrum. The first one is the determination of the energy Green's function and this is presented in Appendix B. The second one is the proof that the spectrum is a power law up to the exponential cutoff; this is done in Appendix C.

B. THE SOLUTION OF THE ENERGY EQUATION AND THE EXPANSION COEFFICIENTS OF THE SPACE SOURCE DISTRIBUTION

In this Appendix we obtain the solution of the energy part of the radiative transfer equation (14). This is derived after substituting the factorized expression (A1) for the occupation number into equation (14) and it reads

$$\frac{1}{x^2}\frac{d}{dx}\left[x^4\left(\frac{dN_k}{dx}+N_k\right)\right]-\delta x\frac{dN_k}{dx}=\gamma_k N_k-g(x)\ , \tag{B1}$$

where $g(x)$ is the spectral part of source function. The boundary conditions are

$$x^3 N_k \to 0 \ \text{ when } \ x\to 0 \ \text{ or } \ x\to\infty\ . \tag{B2}$$

In order to find the Green's function $G_k(x,x_0)$, the spectral part of the source function $g(x)$ is assumed to be proportional to a delta function, i.e.,

$$g(x)=\delta(x-x_0)/x^3\ , \tag{B3}$$

and the differential operator of equation (B1) should be rewritten in the self-adjoint form $(d/dx)[p(x)(d/dx)]$. The integrating factor $f(x)=e^x x^{2-\delta}$ allows us to get such a form [i.e., $p(x)=x^2 f(x)$] with $p(x)=e^x x^{4-\delta}$. The reduction of equation (B1) to the self-adjoint form is followed by integration of the left and right side of the equation from x_{0-} to x_{0+} and thus the constant D of the symmetric form of the Green's function is obtained (see below). The Green's function is given by

$$G_k(x,x_0)=\begin{cases} DN_1(x)N_2(x_0), & \text{if } x\le x_0;\\ DN_1(x_0)N_2(x), & \text{if } x\ge x_0,\end{cases} \tag{B4}$$

where $N_1(x)$ and $N_2(x)$ are the solutions of the homogeneous equation (B1) [i.e., with $g(x)\equiv 0$]. The solutions $N_1(x)$ and $N_2(x)$ satisfy the boundary conditions (B2) at $x\to 0$ and $x\to\infty$ respectively. Hence the constant D, expressed through the Wronskian,

$$W[N_1(x_0),N_2(x_0)] \ = \ N_1(x_0)N_2'(x_0)-N_1'(x_0)N_2(x_0)\ , \tag{B5}$$

reads

$$D \;=\; -\frac{f(x_0)}{x_0^3 p(x_0) W[N_1(x_0), N_2(x_0)]} \;. \tag{B6}$$

The solutions $N_1(x)$ and $N_2(x)$ are expressed in terms of the Whittaker functions (Abramowitz & Stegun 1970) as

$$N_1(x) = x^{(\delta-4)/2} e^{-x/2} M_{2+\delta/2,[(\delta-3)^2+4\gamma_k]^{1/2}/2}(x) \;, \tag{B7}$$

and

$$N_2(x) = x^{(\delta-4)/2} e^{-x/2} W_{2+\delta/2,[(\delta-3)^2+4\gamma_k]^{1/2}/2}(x) \;. \tag{B8}$$

The product of $p(x_0)W[N_1(x_0), N_2(x_0)]$ is independent of x_0 and is equal to $-\Gamma(2\alpha_k + 4 + \delta)/\Gamma(\alpha_k)$. In the limit of low energy source photons ($x_0 \ll 1$), the Green's function $G_k(x, x_0)$ is transformed into equation (22).

The expansion coefficients c_k of the space source photon distribution $S(\tau)$, where $j/\kappa c = S(\tau)g(x)/x^3$ (see eq. [14]), are determined by using the orthogonality of the eigenfunctions (A3). Thus we obtain

$$c_k = \int_0^{\tau_b} [e^{-\tau}\Phi(-\lambda_k^2 + 5/2, 7/2, \tau)S(\tau)]d\tau / H_k(\tau_b) \;, \tag{B9}$$

where

$$H_k(\tau_b) = \int_0^{\tau_b} d\tau e^{-\tau} \tau^{5/2} \Phi^2(-\lambda_k^2 + 5/2, 7/2, \tau) \;. \tag{B10}$$

C. THE ASYMPTOTIC FORM OF THE ENERGY GREEN'S FUNCTION

In order to study the asymptotic form of the solution (21) when $kT_e \ll m_e c^2$, the integral of equation (22) should be calculated for indices $\omega = \delta + 3 + \alpha_1 \gg 1$ by the steepest descend method. Introducing a new integration variable $t' = t\alpha$, the integral

$$J(x, \alpha, \omega) = \int_0^\infty e^{-t'}(x + t')^\omega t'^{\alpha-1} dt' \ , \tag{C1}$$

is rewritten in the form

$$J(x, \alpha, \omega) = \alpha^\alpha \int_0^\infty \exp\left[-\varphi(t)\right] \frac{dt}{t} \ . \tag{C2}$$

Here and below the subscript 1 is omitted for simplicity. The exponent of the integrand in equation (C2),

$$\varphi(t) = \alpha[t - \frac{\omega}{\alpha} \ln(x + \alpha t) - \ln t] \ , \tag{C3}$$

has a maximum at

$$t_0 = \frac{\omega + \alpha - x + [(\omega + \alpha - x)^2 + 4x\alpha]^{1/2}}{2\alpha} \ . \tag{C4}$$

The second derivative of $\varphi(t)$ is

$$\varphi''(t) = \alpha \left[\frac{\omega\alpha}{(x + \alpha t)^2} + \frac{1}{t^2} \right] \ . \tag{C5}$$

Finally the integral $J(x, \alpha, \omega)$ is given by the steepest descend formula

$$J(x, \alpha, \omega) = \alpha^\alpha \frac{\exp[-\varphi(t_0)]}{t_0} \left[\frac{2\pi}{\varphi''(t_0)} \right]^{1/2} \ . \tag{C6}$$

This formula provides very high accuracy for any index $\alpha > 1$, but for $\alpha \leq 1$ the integral should be transformed by using integration by parts as follows

$$J(x, \alpha, \omega) = [J(x, \alpha + 1, \omega) - \omega J(x, \alpha + 1, \omega - 1)]/\alpha \ . \tag{C7}$$

¿From the above we find that

$$J(x, \alpha, \omega) = e^x \Gamma(\omega + \alpha) = e^x \Gamma(2\mu) \ , \qquad \text{for} \ \ x < \omega \ , \tag{C8}$$

and

$$J(x,\alpha,\omega) = \Gamma(\alpha)x^{\omega+3+\alpha} \ , \qquad \text{for} \ \ x > \omega \ . \tag{C9}$$

Thus, the spectral energy power law $E^{-\alpha}$ extends up to a high energy cutoff. Beyond this energy, the spectrum falls off exponentially (or has a hump) of the the form $C_h x^{\delta+3} \exp\left(-E/kT_e\right)$.

D. ENERGY GAIN AND LOSS PER SCATTERING

There is a standard procedure to estimate the energy gain and loss per scatering (e.g., Prasad et al. 1988). In order to make these estimates one has to find the response of the energy operator of the kinetic equation (see eq. [14]) to a delta-function injection of photons. The dimensionless photon energy density in this case is $x^3 n = x\delta(x - x_0)$, where $x = E/kT_e$, E is the photon energy, T_e is the temperature of the electrons and n is the occupation number. The energy change per scattering Δx can then be found by multiplification of the kinetic equation by x^3 and integration over x. Thus we have

$$\Delta x = \int_0^\infty \left\{ -\frac{1}{\dot{m}} x^4 \frac{\partial n}{\partial x} + x\Theta f_b \frac{\partial}{\partial x} \left[x^4 \left(f_b^{-1} n + \frac{\partial n}{\partial x} \right) \right] \right\} dx \ , \tag{D1}$$

where $f_b = 1 + (v_b/c)^2/(3\Theta)$, and $\Theta = kT_e/m_e c^2$. Integration by parts gives

$$\Delta x = \left[\frac{4}{\dot{m}} + 4[\Theta + (v_b/c)^2/3] \right] \int_0^\infty x^3 n dx - \Theta \int_0^\infty x^4 n dx \ . \tag{D2}$$

Substituting $x^3 n = x\delta(x - x_0)$ in this equation we obtain

$$\Delta x = \left[\frac{4}{\dot{m}} + 4[\Theta + (v_b/c)^2/3] - \frac{E_0}{m_e c^2} \right] x_0 \ , \tag{D3}$$

where E_0 is the photon energy before scattering and $x_0 = E_0/kT_e$. The first term on the right hand side of equation (D3) is the Comptonization to first order in the electron bulk velocity, the second term is to second order in the electron velocity (thermal and bulk) and the third term gives the photon energy loss due to the recoil of the electron.

E. SEPARATION OF VARIABLES

We remind the reader how the method of separation of variables works in the case of a general linear operator equation of the form

$$L_x n + L_\tau n = S(\tau)g(x), \quad \text{for} \;\; 0 \le \tau \le \tau_b \;\; \text{and} \;\; 0 < x < \infty, \tag{E1}$$

with boundary conditions $l_o n = 0$ at $\tau = 0$ and $l_{\tau_b} n = 0$ at $\tau = \tau_b$, where τ and x are the space and energy variables respectively, and the boundary operators l_o, l_{τ_b} are independent of the energy variable (in the case considered in our present paper, l_{τ_b} depends on energy). The eigenfunction $R_k(\tau)$ of the space operator ($L_\tau R_k + \lambda_k^2 R = 0$, $l_o R_k = l_{\tau_b} R_k = 0$) always exists for the very wide class of operators considered in equation (E1). The eigenfunctions form a complete set, i.e., the space part of the source function $S(\tau)$ can be expanded in a series $S(\tau) = \Sigma c_k R_k(\tau)$, with c_k the expansion coefficients. Having in mind this expansion and also that $n(\tau, x)$ is looked for as a series

$$n(\tau, x) = \sum_{k=1}^{\infty} c_k R_k(\tau) N_k(x) \;, \tag{E2}$$

where $N_k(x)$ is the spectrum of the k-mode of the solution, one can see that the whole problem is reduced to the solution of the equation for the k-energy component $N_k(x)$. Namely,

$$\Sigma c_k R_k(\tau)[L_x N_k - \lambda_k^2 N_k - g(x)] = 0, \tag{E3}$$

from which one obtains

$$L_x N_k - \lambda_k^2 N_k - g(x) = 0, \tag{E4}$$

because of completeness of the $\{R_k(\tau)\}$.

In general, when the internal boundary operator $l_{\tau_b}^x$ depends on energy (as it is in our case, see eqs. [16, 19]), the above method of separation of variables cannot be applied. But in the particular case of BP81a (their eq. [18]; see also our eq. [14] with $\delta_b = \delta$), a power

law is a solution in the range of dimensionless energies $x_0 < x < \delta$ ($x_0 \ll 1$, $1 \ll \delta$). This can be checked by simple substitution of the product $R(\tau)x^{-\alpha}$ into equation (14) (where δ_b has to be replaced by δ) and into the boundary conditions (eqns. [17] and [19]). After substitution we get a system of equations for the determination of the spectral index α. In addition, we assume that the photon source spectrum $g(x)$ has characteristic energies much less than m_ec^2 (for example, for a δ-function energy injection, $g(E) = \delta(E - E_0)$ and $E_0 \ll m_ec^2$), and therefore there are no source photons with $E \gg E_0$. Thus, instead of equation (E4), we get in this case

$$L_x x^{-\alpha} - \lambda^2 x^{-\alpha} = (\lambda_\alpha^2 - \lambda^2)x^{-\alpha} = 0,$$

or

$$\lambda_\alpha^2 - \lambda^2 = 0, \tag{E5}$$

for $x > x_0$ and where λ_α^2 is the eigenvalue of the operator L_x. The internal boundary operator $l_{\tau_b}^x$ is a linear differential operator with respect to the variables τ and x. The power law $x^{-\alpha}$ is an eigenfunction of this operator, namely $l_{\tau_b}^x x^{-\alpha} = l_{\tau_b}^\alpha x^{-\alpha}$. Thus

$$l_{\tau_b}^x x^{-\alpha} R(\tau) = [l_{\tau_b}^\alpha R(\tau)]x^{-\alpha} = 0 \qquad \text{at} \qquad \tau = \tau_b,$$

or

$$l_{\tau_b}^\alpha R(\tau) = 0 \qquad \text{at} \qquad \tau = \tau_b, \tag{E6}$$

and

$$l_o R(\tau) = 0 \qquad \text{at} \qquad \tau = 0. \tag{E7}$$

As it is proved in Appendix C, a power law is an eigenfunction of the operator L_x for energies up to a high energy cutoff. Combining equation $L_\tau R + \lambda^2 R = 0$ and equations (E5)-(E7) we get a complete system of equations for the determination of the spectral index α, the eigenvalue λ^2 and the eigenfunction. Practically, the correctness of this approach

can be clearly seen from Figure 2, where the numerical and the analytical solutions are compared.

It is not our goal to go into the deep mathematical details about the uniqueness of this solution. We can only remind the reader that there is a general theorem for the existence and uniqueness of the solution for the boundary problem of the partial differential equation of the second order. This theorem is valid for a wide class of differental operators L_x, L_τ, $l^x_{\tau_b}$, l_o.

REFERENCES

Abramowitz, M., & Stegun, L. 1970, Handbook of Mathematical Functions (New York: Dover)

Begelman, M. C. 1979, MNRAS, 187, 237

Bekker, P. A. 1988, ApJ, 327, 772

Blandford, R. D., & Payne, D. G. 1981a, MNRAS, 194, 1033 (BP81a)

———— . 1981b, MNRAS, 194, 1041 (BP81b)

Colpi, M. 1988, ApJ, 326, 223 (C88)

Hua, X. M., & Titarchuk, L. G. 1995, ApJ, 449, 188

Lyubarskij, Yu. E., & Sunyaev, R. A. 1982, Sov. Astr. Letters, 8, 330 (LS82)

Mastichiadis, A., & Kylafis, N. D. 1992, ApJ, 384, 136 (MK92)

Payne, D. G., & Blandford, R. D. 1981, MNRAS, 196, 781 (PB81)

Prasad, M. K., Shestakov, A. I., Kershaw, D. S., & Zimmerman, G. B. 1988, J. Quant. Spectrosc. Radiat. Transfer, 40, 29

Press, W. H., Teukolsky, S. A., Vetterling, W. T., & Flannery, B. P. 1992, Numerical Recipies (Cambridge: Cambridge University Press)

Psaltis, D., & Lamb, F. K. 1996, ApJ, submitted

Rees, M. J. 1978, Phys. Scripta, 17, 193

Riffert, H. 1988, ApJ, 327, 760

Sobolev, V. V. 1975, Light Scattering in Atmospheres (Oxford: Pergamon)

Sunyaev, R. A. & Titarchuk, L. G. 1980, A&A, 86, 121

——————— 1985, A&A, 143, 374

Titarchuk, L. G. & Lyubarskij, Yu. E. 1995, ApJ, 450, 876

Titarchuk, L. G., Mastichiadis, A. & Kylafis, N. D. 1996, A&A Suppl 120, C171

This manuscript was prepared with the AAS LaTeX macros v4.0.

Fig. 1.— Plot of the emergent spectral energy flux versus photon energy for $\dot{m} = 3$, $kT_e = 1$ keV, $kT_{bb} = 1$ keV, $A = 0$, $\mu = 0.3$ and the radiative transfer equation is solved numerically. The dashed line is for the case where the second order bulk effect is excluded (see BP81a, their eq. [15]), while the solid line includes this effect (eq. [14] of the present paper).

Fig. 2.— Plot of the emergent spectral energy flux versus photon energy. The solid line is identical to the dashed one in Figure 1, while the dashed line corresponds to the approximate analytic solution.

Fig. 3.— Plot of the emergent spectral energy flux versus photon energy. Here $kT_e = 2.5$ keV, $A = 0$, $T_e/T_{bb} = 3$, $\dot{m} = 3$. The emergent spectrum is calculated as a convolution of series (21) with a blackbody source distribution. The space source distribution is given by equation (20) with $S_0 = 1$ and $\mu = 0.3$. The solid line is the emergent spectrum. The dashed lines represent the contributions to the spectrum by the first nine terms of series.

Fig. 4.— a) Plot of the emergent spectral energy flux versus photon energy for a monochromatic injection at energy $E_0 = 10^{-4} kT_e$ and for three different space source distributions. Curve 1 is for a space source distribution proportional to the first eigenfunction. Curves 2 and 3 are for the space source distribution given by equation (20) with $\mu = 1$ and $\mu = 0.3$ respectively. The other parameters are the same as in Figure 3.
b) Same as in a), but for a blackbody input spectrum with $kT_{bb} = 0.833$ keV.

Fig. 5.— Plot of the first four eigenvalues as functions of the accretion rate $\dot{m}$ in the case of $A = 0$, $kT_e = 1$ keV and $r_b = r_s$. The solid curves correspond to λ_1^2, λ_2^2, λ_3^2 and λ_4^2 from bottom to top. The dashed curve gives the approximate analytic value of λ_1^2.

Fig. 6.— a) Plot of the energy spectral index α_1 versus $\dot{m}$ for $r_b = r_s$ and $kT_e = 0.01$ keV (solid line), $kT_e = 1$ keV (dotted line) and $kT_e = 3$ keV (dashed line).
b) Plot of the energy spectral index α_1 versus $\dot{m}$ for different values of the albedo A. Here

$kT_e = 1$ keV, $r_b = r_s$ and A equal to 0 (solid line), 0.5 (dotted line) and 1 (dashed line).

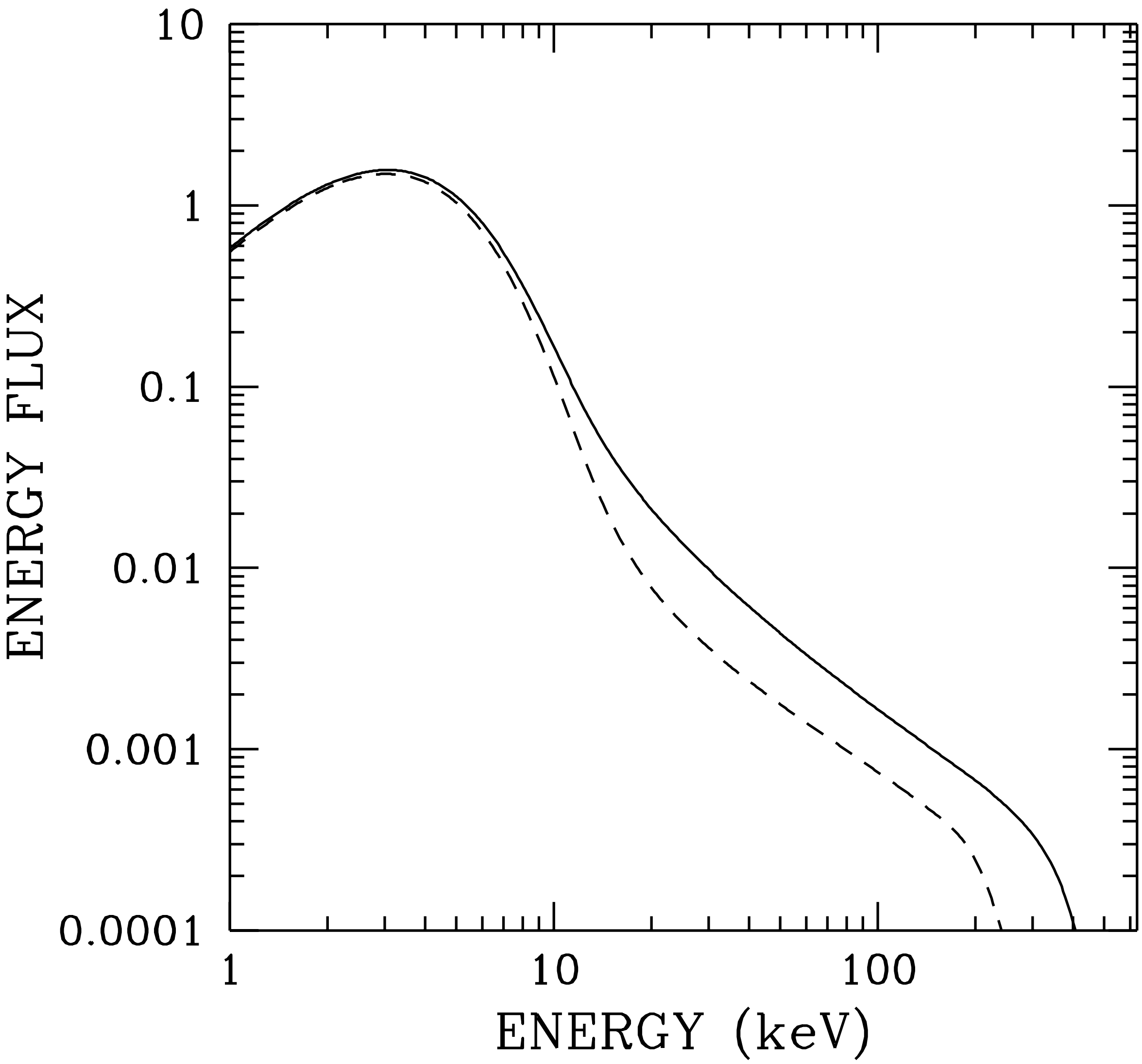
10
1
0.1
0.01
0.001
0.0001
ENERGY FLUX
1
10
100
ENERGY (keV)

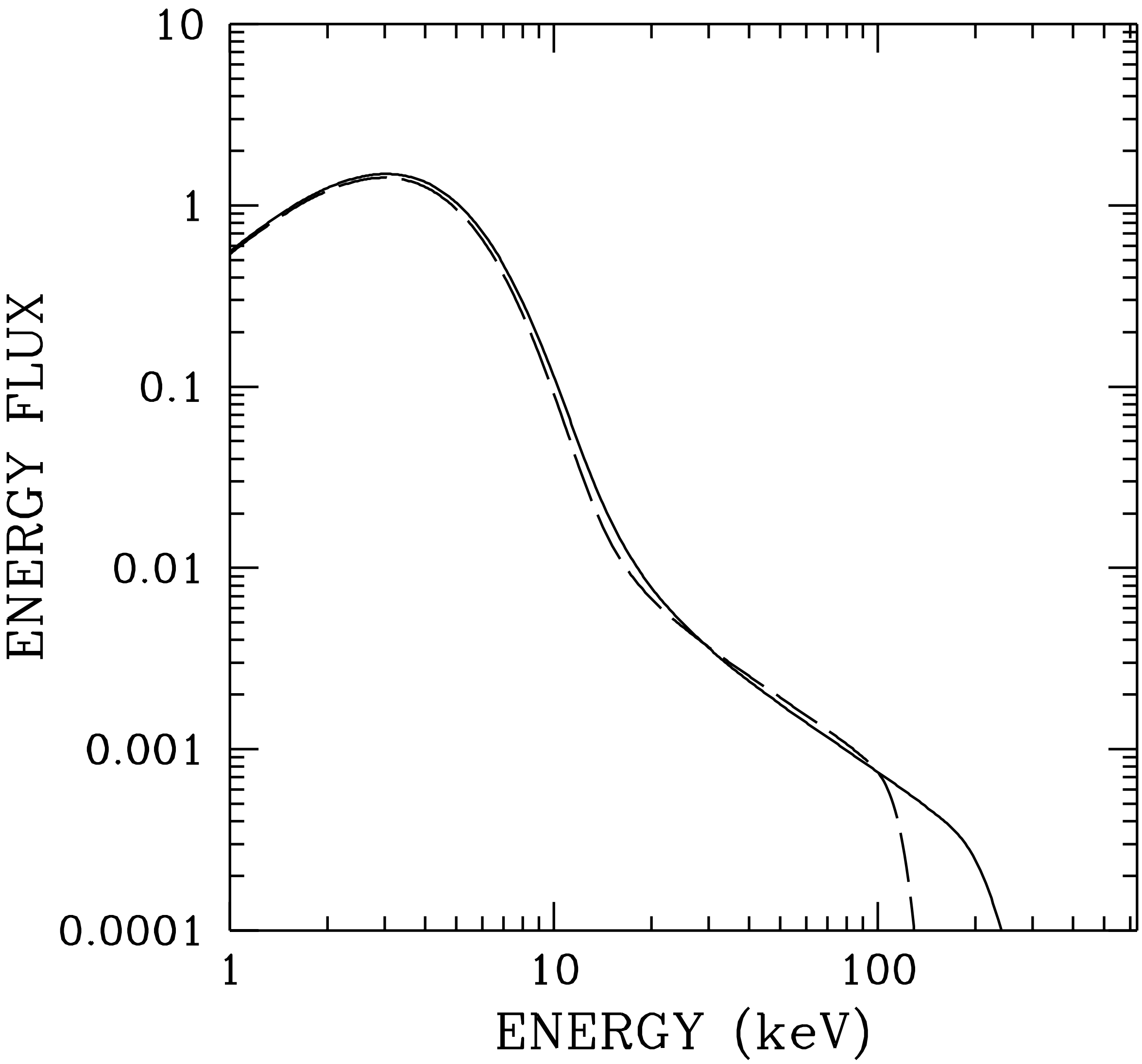

10
1
0.1
0.01
0.001
0.0001
1
10
100
ENERGY FLUX
ENERGY (keV)

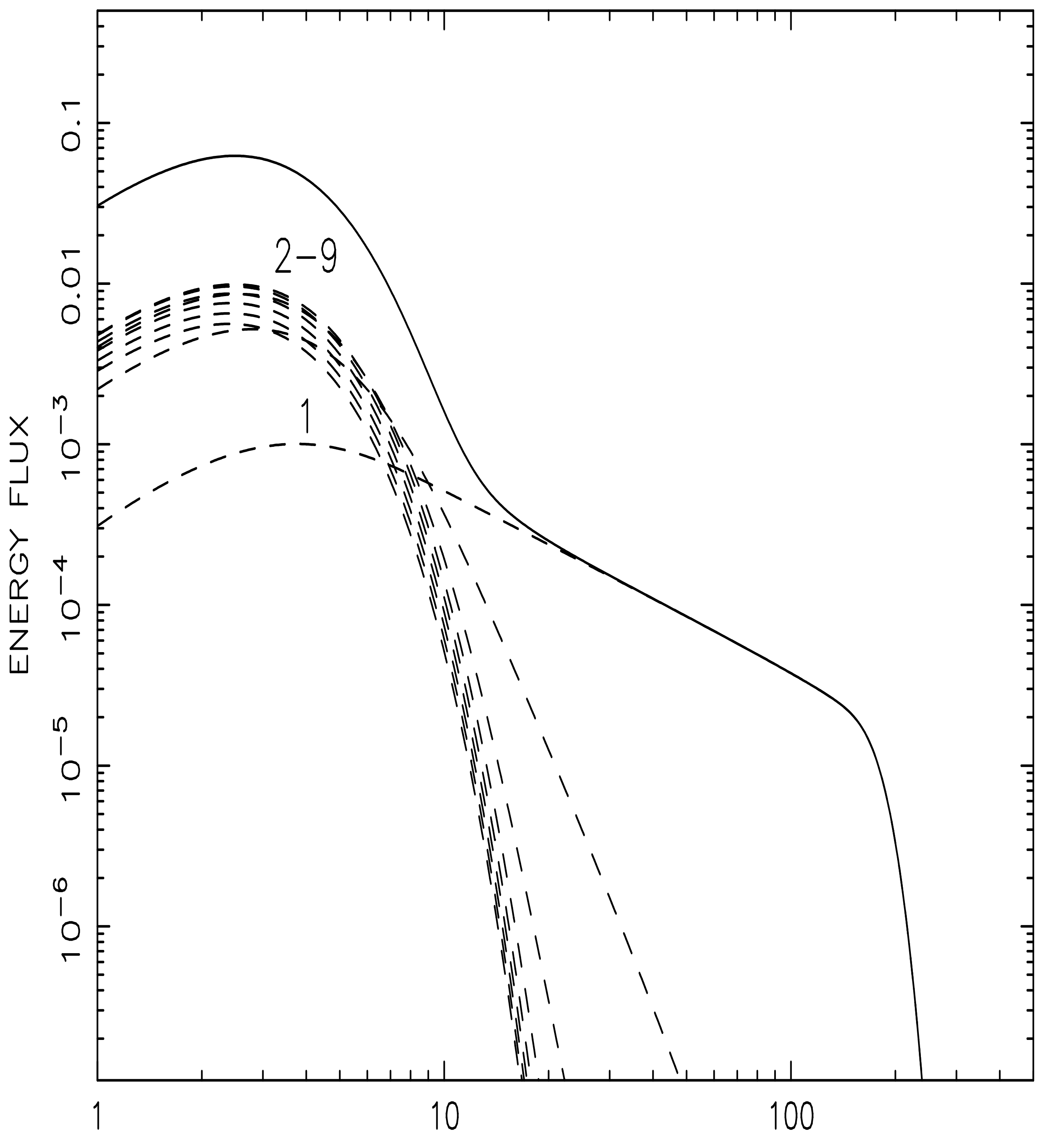

ENERGY FLUX
0.1
0.01
10^{-3}
10^{-4}
10^{-5}
10^{-6}
1
10
100
ENERGY (keV)
2-9
1

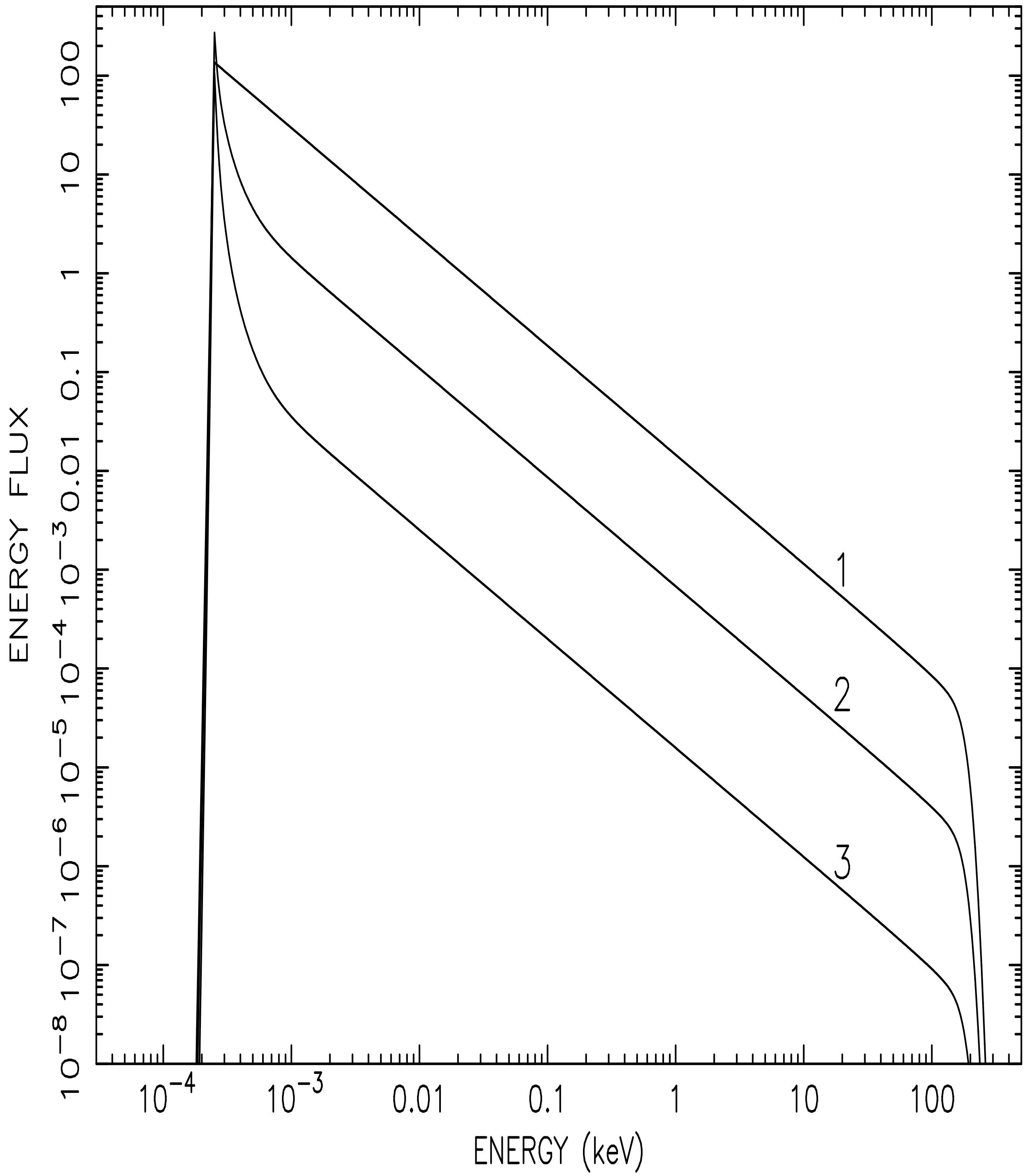

ENERGY FLUX
10^{-8}
10^{-7}
10^{-6}
10^{-5}
10^{-4}
10^{-3}
0.01
0.1
1
10
100
1
2
3
10^{-4}
10^{-3}
0.01
0.1
1
10
100
ENERGY (keV)

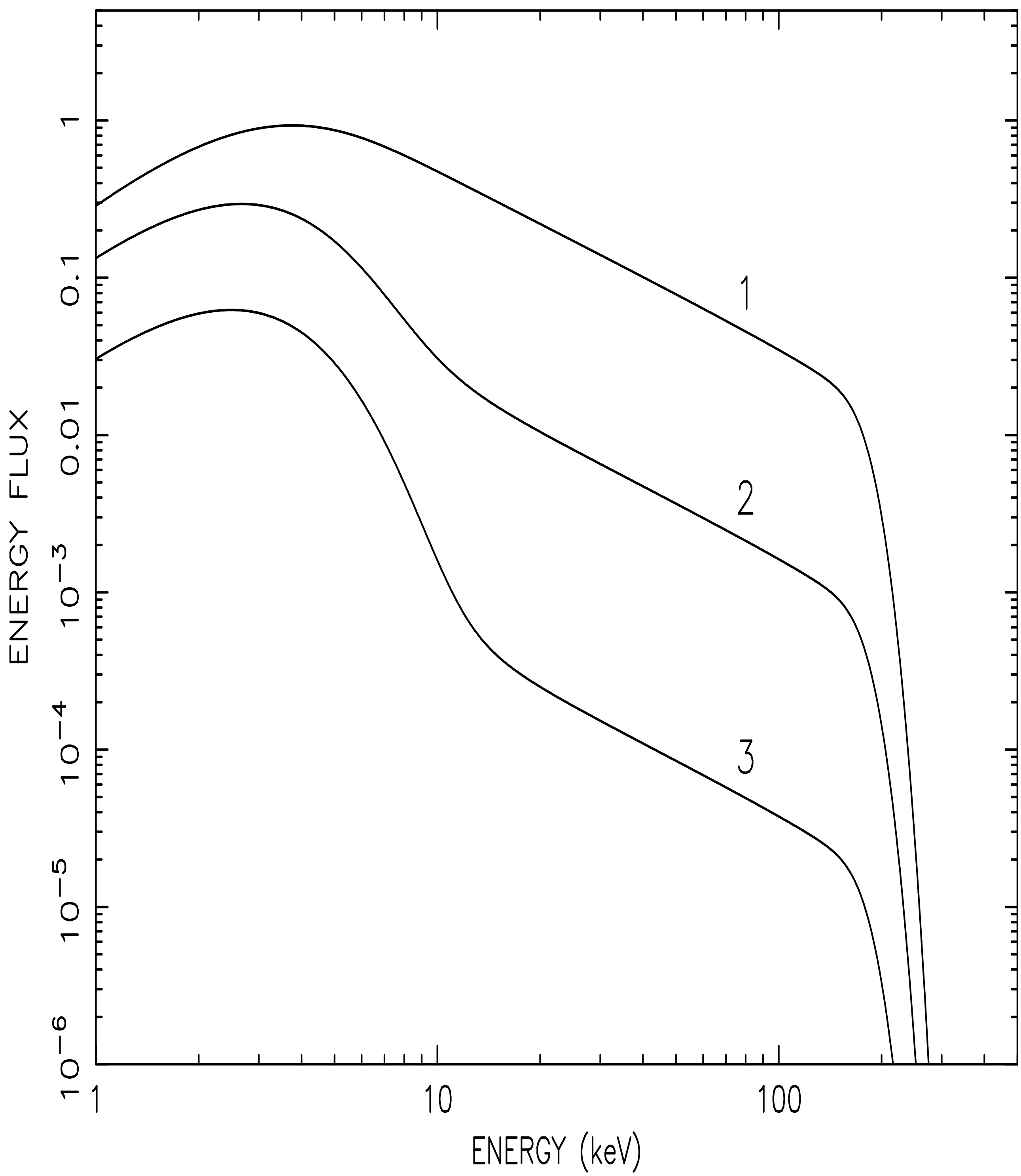
ENERGY FLUX
ENERGY (keV)
1
0.1
0.01
10^{-3}
10^{-4}
10^{-5}
10^{-6}
1
10
100
1
2
3

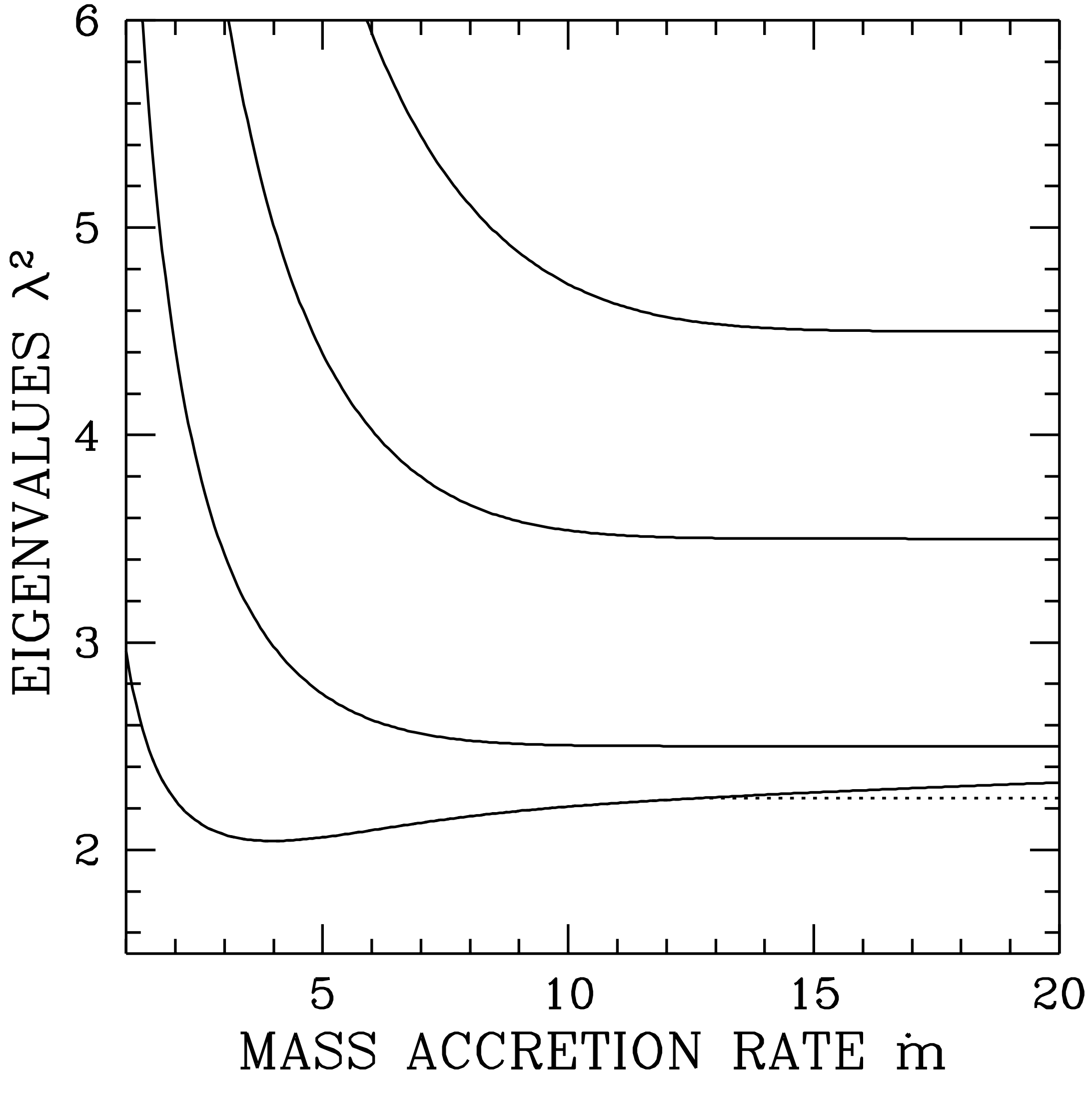
6
5
4
3
2
5
10
15
20
EIGENVALUES λ^2
MASS ACCRETION RATE $\dot{m}$

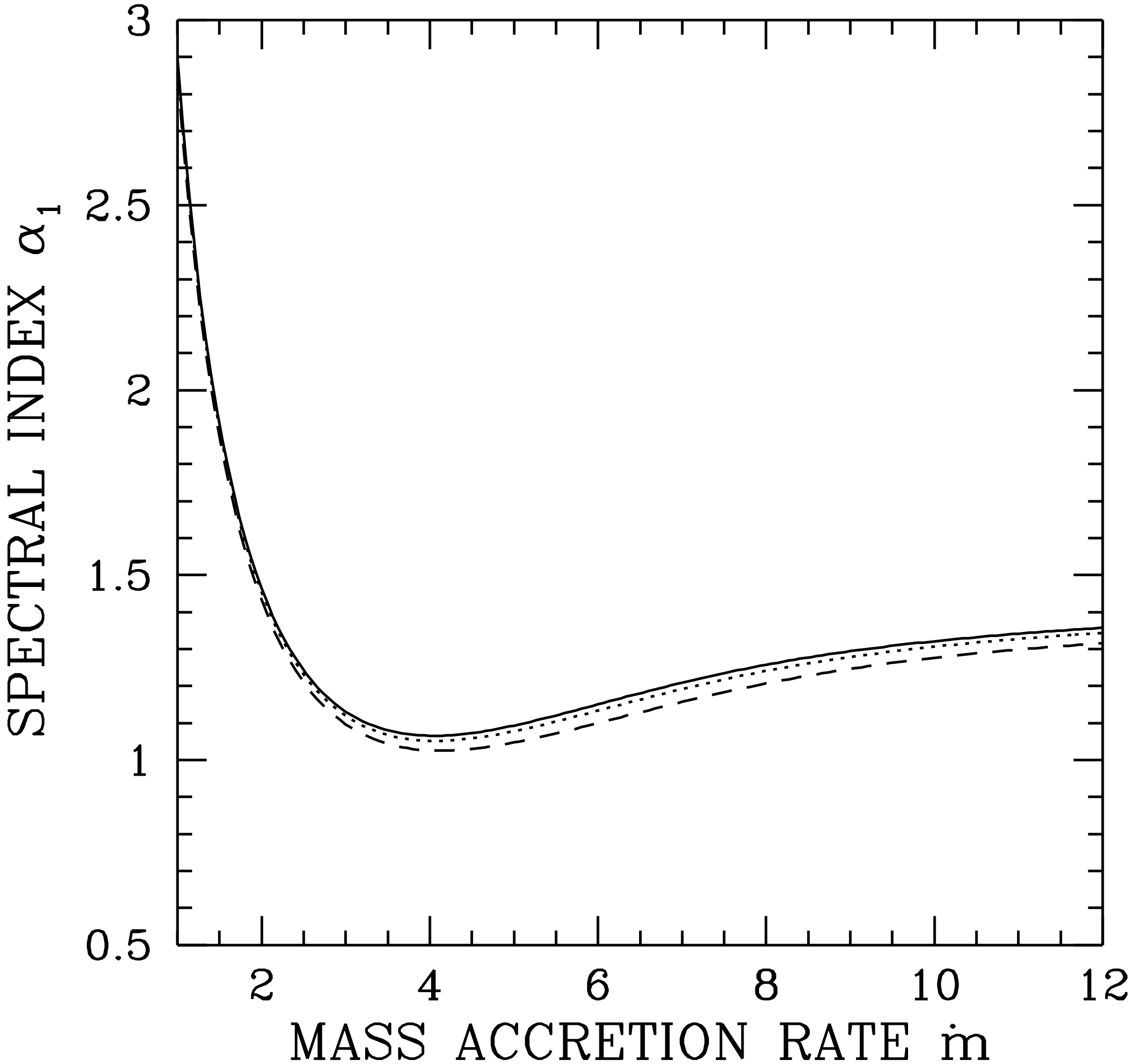

3
2.5
2
1.5
1
0.5
2
4
6
8
10
12
SPECTRAL INDEX α_1
MASS ACCRETION RATE $\dot{m}$

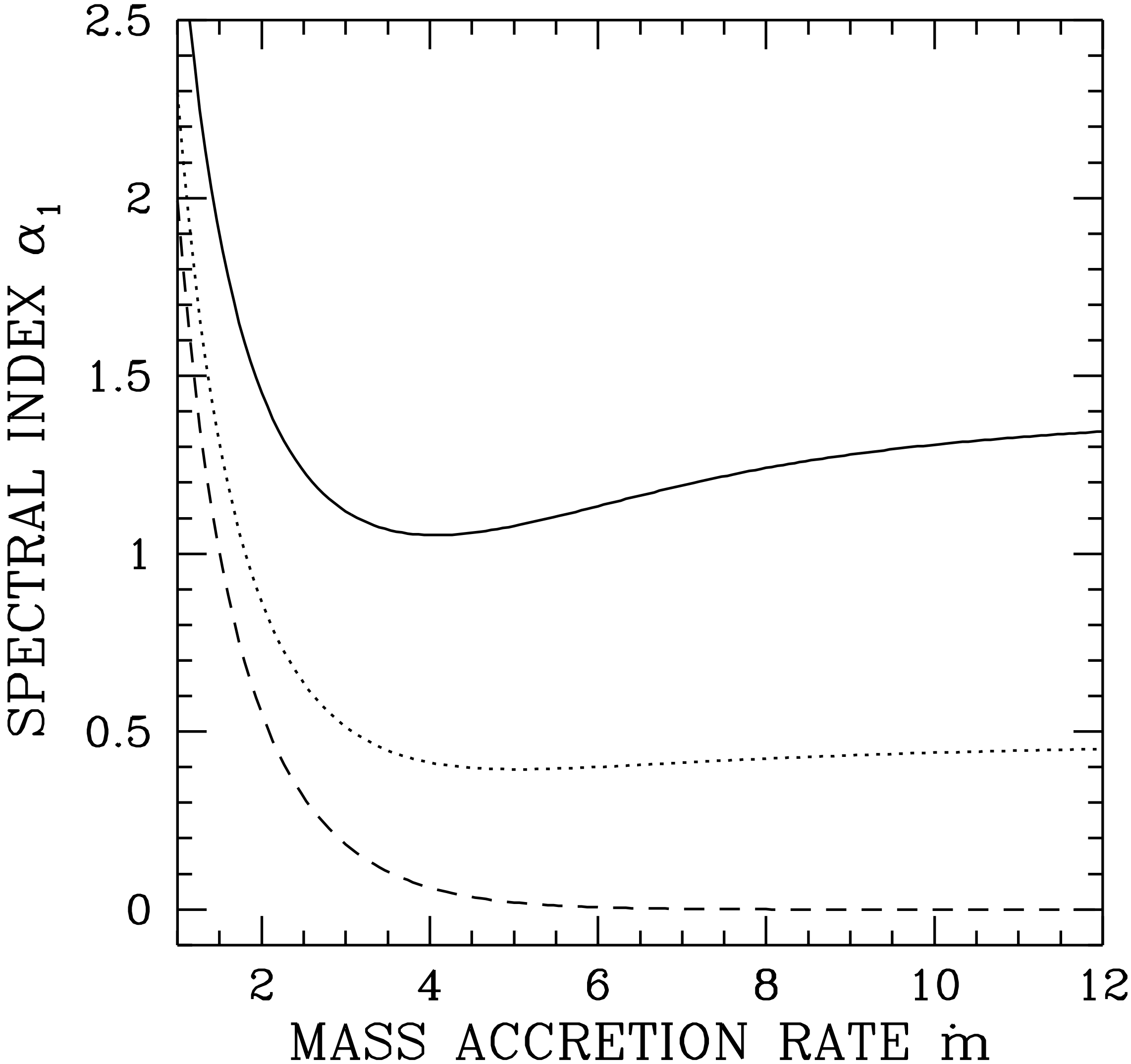

2.5
2
1.5
1
0.5
0
2
4
6
8
10
12
SPECTRAL INDEX α_1
MASS ACCRETION RATE $\dot{m}$